J|A|C|S
ARTICLES
Published on Web 04/13/2007

Correlation of Protein Structure and Dynamics to Scalar Couplings across Hydrogen Bonds

Hans-Jürgen Sass,*,† Franziska Fang-Fang Schmid,‡ and Stephan Grzesiek*,†

Biozentrum and Department Chemie, University of Basel, Klingelbergstrasse 50, 4056 Basel, Switzerland

Received November 21, 2006; E-mail: stephan.grzesiek@unibas.ch; juergen.sass@unibas.ch

Abstract: NMR-observable scalar couplings across hydrogen bonds in nucleic acids and proteins present a quantitative measure for the geometry and − by the implicit experimental time averaging − dynamics of hydrogen bonds. We have carried out in-depth molecular dynamics (MD) simulations with various force fields on three proteins: ubiquitin, the GB1 domain of protein G, and the SMN Tudor domain, for which experimental $^{h3}J_{NC'}$ scalar couplings of backbone hydrogen bonds and various high-resolution X-ray structures are available. Theoretical average values for $^{h3}J_{NC'}$ were calculated from the snapshots of these MD simulations either by density functional theory or by a geometric parametrization (Barfield, M. *J. Am. Chem. Soc.* **2002**, *124*, 4158−4168). No significant difference was found between the two methods. The results indicate that time-averaging using explicit water solvation in the MD simulations improves significantly the agreement between experimental and theoretical values for the lower resolution structures ubiquitin (1.8 Å), Tudor domain (1.8 Å), and protein G (2.1 Å). Only marginal improvement is found for the high-resolution structure (1.1 Å) of protein G. Hence, experimental $^{h3}J_{NC'}$ values are compatible with a static, high-resolution structural model. The MD averaging of the low-resolution structures moves the averages of the r_{HO} distance and the H···O═C angle θ closer to their respective values in the high-resolution structures, thereby improving the agreement using experimental $^{h3}J_{NC'}$ data. In contrast, MD averaging with implicit water models deteriorates the agreement with experiment for all proteins. The differing behavior can be explained by an artifactual lengthening of H-bonds caused by the implicit water models.

Introduction

The NMR detection of electron-mediated scalar couplings across hydrogen bonds (H-bonds) in nucleic acids[1] and proteins[2] makes it possible to study fine details of the behavior of H-bonds in biomolecules.[3] As the size of the couplings depends quadratically on the electronic wave function overlap within the H-bond, there is a very strong dependence on H-bond geometries. In particular, an exponential dependence on H-bond lengths was established experimentally[4] and by density functional theory (DFT) calculations.[5,6] The latter also prove the dependence on several H-bond angles.

Guided by insights from a linear combination of atomic orbitals/sum-over-states (LCAO/SOS) analysis, the geometric dependencies for $^{h3}J_{NC'}$ couplings in N−H···O═C H-bonds of proteins have been parametrized[6] to good approximation by several simple geometric formulas; the simplest one being

$$^{h3}J_{NC} = (-357\ \text{Hz}) \exp(-3.2 r_{HO}/\text{Å}) \cos^2\theta \qquad (1)$$

where θ represents the H···O═C angle. (Equation 1 slightly differs from the original eq 10 given by Barfield[6] by the omission of a nonphysical small constant offset of 0.04 Hz and the readjustment of the amplitude from −360 to −357 Hz, which gave slightly better agreement to our DFT data presented below.)

It is obvious that the experimentally observed H-bond scalar couplings represent time averages over the motions of H-bonds up to a time that is determined by the inverse of the coupling constants and the total time used for magnetization transfer, that is, about 0.1−1 s. Thus the question arises whether the dynamics of proteins has an influence on the observed $^{h3}J_{NC'}$ couplings. Recently, Sattler and co-workers[7] observed that the agreement between DFT-derived and experimentally observed $^{h3}J_{NC'}$ couplings in the SMN Tudor domain protein can be improved, when the couplings are calculated as an average over the

† Biozentrum.
‡ Department Chemie.

(1) (a) Dingley, A.; Grzesiek, S. *J. Am. Chem. Soc.* **1998**, *120*, 8293−8297. (b) Pervushin, K.; Ono, A.; Fernandez, C.; Szyperski, T.; Kainosho, M.; Wüthrich, K. *Proc. Natl. Acad. Sci. U.S.A.* **1998**, *95*, 14147−14151.
(2) (a) Cordier, F.; Grzesiek, S. *J. Am. Chem. Soc.* **1999**, *121*, 1601−1602. (b) Cornilescu, G.; Hu, J. S.; Bax, A. *J. Am. Chem. Soc.* **1999**, *121*, 2949−2950.
(3) Grzesiek, S.; Cordier, F.; Jaravine, V.; Barfield, M. *Prog. Nucl. Magn. Reson. Spectrosc.* **2004**, *45*, 275−300.
(4) Cornilescu, G.; Ramirez, B. E.; Frank, M. K.; Clore, G. M.; Gronenborn, A. M.; Bax, A. *J. Am. Chem. Soc.* **1999**, *121*, 6275−6279.
(5) (a) Dingley, A. J.; Masse, J. E.; Peterson, R. D.; Barfield, M.; Feigon, J.; Grzesiek, S. *J. Am. Chem. Soc.* **1999**, *121*, 6019−6027. (b) Benedict, H.; Shenderovich, I. G.; Malkina, O. L.; Malkin, V. G.; Denisov, G. S.; Golubev, N. S.; Limbach, H. H. *J. Am. Chem. Soc.* **2000**, *122*, 1979−1988. (c) Barfield, M.; Dingley, A. J.; Feigon, J.; Grzesiek, S. *J. Am. Chem. Soc.* **2001**, *123*, 4014−4022. (d) Del Bene, J. E.; Perera, S. A.; Bartlett, R. *J. Magn. Reson. Chem.* **2001**, *39*, S109−S114. (e) Bryce, D. L.; Wasylishen, R. E. *J. Biomol. NMR* **2001**, *19*, 371−375. (f) Scheurer, C.; Brüschweiler, R. *J. Am. Chem. Soc.* **1999**, *121*, 8661−8662. (g) Bagno, A. *Chem. Eur. J.* **2000**, *6*, 2925−2930.
(6) Barfield, M. *J. Am. Chem. Soc.* **2002**, *124*, 4158−4168.
(7) Markwick, P. R. L.; Sprangers, R.; Sattler, M. *J. Am. Chem. Soc.* **2003**, *125*, 644−645.

10.1021/ja068336h CCC: $37.00

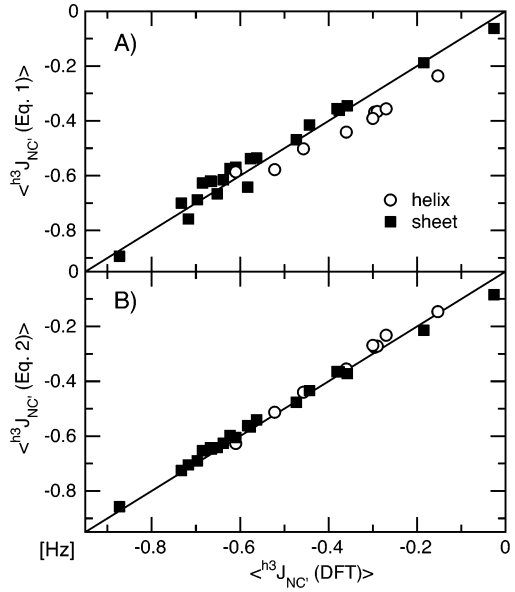

Figure 1. Comparison of MD averages over $^{h3}J_{NC'}$ couplings calculated by geometric parametrizations[6] or by DFT. The values are averages over a 0.5-ns MD trajectory of ubiquitin with explicit water solvation. Comparisons are shown for the geometric parametrization according to (A) eq 1 or (B) eq 2 for H-bonds in (○) α-helical or (■) sheet conformations.

snapshots of a 0.5-ns molecular dynamics (MD) trajectory instead of using the coordinates from a static X-ray or NMR structure.

Here we have reinvestigated this correlation between protein dynamics and H-bond couplings for three proteins: ubiquitin, the GB1 domain of protein G, and the SMN Tudor domain, for which experimental $^{h3}J_{NC'}$ scalar couplings of backbone hydrogen bonds and X-ray structures at various resolutions are available. In particular, we have studied the influence of the X-ray resolution, MD force fields, and water models on the accuracy of the predictions. The results indicate that MD averaging using explicit water models significantly improves the agreement between predicted and experimental $^{h3}J_{NC'}$ for lower resolution structures but not for the very high-resolution structure of protein G. Thus the experimental $^{h3}J_{NC'}$ values are compatible with a static structural model.

Results

Comparison of MD Averaging of DFT-Calculated and Analytically Calculated $^{h3}J_{NC'}$ Couplings. In order to speed up the process of calculating averaged $^{h3}J_{NC'}$ couplings from MD trajectories, it was tested whether geometric parametrizations can be used instead of full DFT calculations. Figure 1A shows a comparison of the $^{h3}J_{NC'}$ averages over the snapshots from a 0.5-ns MD trajectory on ubiquitin that were obtained either by DFT or by use of eq 1. The agreement between both methods is very reasonable and corresponds to a root-mean-square deviation (rmsd) of 0.048 Hz. As pointed out by Barfield,[6] eq 1 leads to small systematic devations between α-helices and β-sheet H-bonds (Figure 1A). This can be improved by taking into account an additional weak dependence on the dihedral angle $\rho = \angle H^N\cdots O'{=}C'{-}N'$:[6]

$$^{h3}J_{NC} = (-366\ \text{Hz})\exp(-3.2r_{HO}/\text{Å})[\cos^2\theta - (0.47\cos^2\rho + 0.70\cos\rho + 0.11)\sin^2\theta] \quad (2)$$

(Equation 2 is obtained from the original eq 12[6] by multiplying out all constant factors.) Use of eq 2 reduces the rmsd to 0.021 Hz (Figure 1B). As the structural dependence of eq 1 is simpler to analyze and the accuracy was sufficient for the present purpose, in the following MD averages were calculated either from this simpler equation or from full DFT calculations.

Static versus Dynamic H-Bonds in Ubiquitin and Protein G. The influence of structural resolution, MD averaging, and energy minimization on the accuracy of the prediction of $^{h3}J_{NC'}$ values was investigated for the three proteins ubiquitin, protein G, and the Tudor domain. Table 1 lists the obtained rmsds relative to the experimental data under various conditions. Figure 2 (top row) shows a comparison between the experimental $^{h3}J_{NC'}$ values and the predictions according to eq 1 by using the static X-ray coordinates for ubiquitin (1ubq, 1.8 Å resolution), protein G (1pga, 2.1 Å), and protein G (2igd, 1.1 Å). Clearly, the accuracy of the prediction increases with improved resolution. Thus the lowest resolution structure (1pga) has the largest deviation (0.316 Hz), whereas the better resolved structures show decreased deviations (1ubq, 0.202 Hz; 2igd, 0.147 Hz).

Using these X-ray structures as starting coordinates, various MD simulations (Table 1) were carried out on ubiquitin and protein G for at least 0.5 ns in explicit water (Tip3P). Subsequently, the $^{h3}J_{NC'}$ couplings were calculated as an average over values obtained by eq 1 from 0.1-ps MD snapshots. The results are shown in Figure 2 (middle row). For the lower resolution structures, the rmsds of these averaged $^{h3}J_{NC'}$ couplings relative to the experimental data decrease significantly as compared to the predictions of the static structures (1ubq, 0.147 Hz; 1pga, 0.141 Hz). However, for the high-resolution structure 2igd, the improvement is only marginal (0.135 Hz). Hence in all three cases, the MD-averaged $^{h3}J_{NC'}$ couplings converge to a very similar rmsd of about 0.14 Hz, which is close to the value obtained from the static high-resolution structure 2igd. This indicates that the experimental data can be reproduced equally well by a static high-resolution structure and that the improvement by the averaging process is related to the quality of the starting coordinates.

As the MD averaging improves the agreement between predicted and measured $^{h3}J_{NC'}$ values for the lower resolution structures, the MD force fields must drive the proteins toward better H-bond geometries. It was therefore of interest whether an improved static structure could be obtained from a simple energy minimization using the same force fields. Figure 2 (bottom) shows the results of such energy minimizations using the respective X-ray structures as starting points. For all three cases, the energy-minimized structures have rmsds in the range of 0.26−0.28 Hz. Thus the energy minimization deteriorates the agreement in all cases besides the lowest resolution structure. Variations of the energy minimization protocol such as using separate minimization of the water or adding an H-bond potential of mean force[8] did not improve this result (data not shown). However, these negative results do not imply that dynamics is necessary to describe the H-bond behavior since the static high-resolution structure reproduces the experimental data equally well.

Variations in H-Bond Geometry during MD Runs. The improvement by the dynamic averaging process for the low-

(8) Grishaev, A.; Bax, A. *J. Am Chem Soc.* **2004**, *126*, 7281−7292.

Table 1. Root-Mean-Square Deviations[a] between Predicted and Experimental $^{h3}J_{NC'}$ Values

	protein G (1.1 Å)	protein G (2.1 Å)	ubiquitin (1.8 Å)	Tudor domain 1[b] (1.8 Å)	Tudor domain 2[c] (1.8 Å)
static (eq 1)	0.147	0.316	0.202	0.325	0.225
static (DFT)	0.149	0.314	0.220		
energy minimized (eq 1)	0.284	0.270	0.260	0.332	0.272
MD avg, explicit water (eq 1)	0.135[d]	0.141[e]	0.147[f]	0.296[f]	0.148[f]
MD[f] avg, explicit water (DFT)			0.141		
MD[f] avg, implicit water generalized Born model (eq 1)	0.253	0.275	0.287	0.067	0.320
MD[f] avg, implicit water SASA model (eq 1)	0.272	0.250	0.309	0.074	0.330
MD[f] avg, implicit water SASA model (DFT)				0.073	0.320

[a] Rms deviations are given in Hertz. [b] $^{h3}J_{NC'}$ experimental data according to Marwick et al.[7] [c] $^{h3}J_{NC'}$ experimental data rescaled by a factor of 2 (see text). [d] MD trajectory 1.25 ns. [e] MD trajectory 1.4 ns. [f] MD trajectory 0.5 ns.

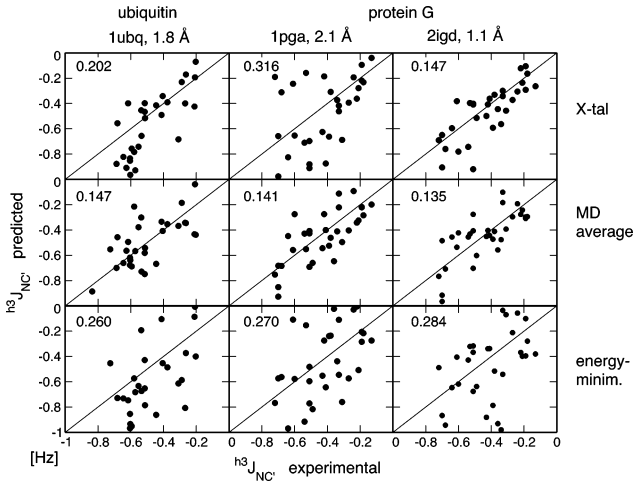

Figure 2. Comparison of experimental and predicted $^{h3}J_{NC'}$ couplings in ubiquitin and protein G. Predictions were calculated from the coordinates of the structures 1ubq (ubiquitin) and 1pga/2igd (protein G). Top row: predictions according to eq 1 using the static X-ray coordinates. Middle row: predictions derived as an MD average according to eq 1 using the X-ray coordinates as starting structure. Bottom row: predictions according to eq 1 using static coordinates that had been obtained from the X-ray structure by energy minimization with the MD force field. Rmsds between experimental and predicted $^{h3}J_{NC'}$ values are indicated in Hertz in the individual panels.

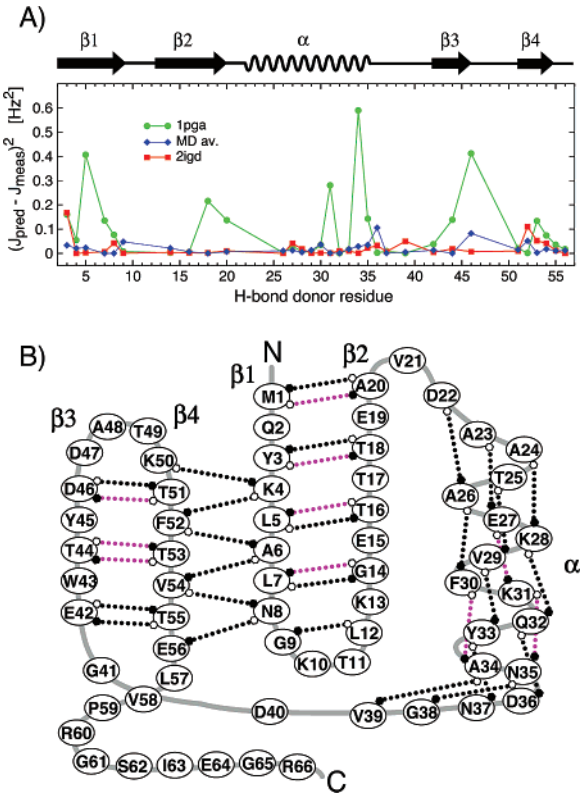

Figure 3. Location of the largest deviations between measured and predicted $^{h3}J_{NC'}$ values in protein G. (A) Squared deviations ($^{h3}J_{NC',predicted} - {}^{h3}J_{NC',measured})^2$ as a function of H-bond donor residue number. Data are shown for predictions according to eq 1 from the static structures 1pga and 2igd, as well as for the average of the MD trajectory with explicit water solvation, which started from the low-resolution structure 1pga. (B) H-Bond topology of protein G. H-bonds highlighted in magenta show particularly strong deviations for the low-resolution structure 1pga in panel A.

resolution structure of protein G can be related to a few particular H-bonds. Figure 3 shows the squared deviations between measured and predicted $^{h3}J_{NC'}$ couplings for the individual H-bonds and a diagram of the H-bond topology of protein G. The predicted $^{h3}J_{NC'}$ couplings are calculated from the structures 1pga (low resolution) and 2igd (high resolution) as well as by MD averaging, which started from the low-resolution structure. For the low-resolution structure, strong deviations are found for H-bonds in the antiparallel sheet $\beta1/\beta2$ (L5→T16, L7→G14, T18→Y3, A20→M1), in the helix (K31→E27, A34→F30, N35→K31), and in the antiparallel sheet $\beta3/\beta4$ (L44→T53, D46→T51, T53→T44). In all cases, the MD averaging improves dramatically the prediction such that it becomes very close to the high-resolution structure. A very similar trend is observed for ubiquitin (data not shown), where the accuracy after averaging improves considerably for the most strongly deviating H-bonds I13→V5, V17→M1, D32→A28, L50→L43, V70→R42.

During MD averaging, the H-bond couplings vary over a wide range. In all MD simulations, the mean standard deviation for individual $^{h3}J_{NC'}$ values was about 0.3 Hz. To understand better the nature of the MD averaging process, the variations of H-bond parameters r_{HO} and θ were investigated for individual H-bonds in protein G. Figure 4 shows corresponding histograms. The mean standard deviations for r_{HO} and θ are 0.24 Å and 11°, respectively. Apparently, the H-bond distance and angle distributions are not uniform and correlate with the secondary structure: whereas β-sheet H-bonds have smaller distance variations and very little correlation between r_{HO} and θ, the profiles for most α-helical H-bonds indicate that smaller angles θ correlate to larger r_{HO} distances. This is particularly pronounced for H-bonds K28→A24, Q32→K28, D36→Q32, which form a connected edge on the exterior side of the α-helix.

Figure 4 also shows the θ and r_{HO} parameters from the static X-ray structures 1pga and 2igd together with their averages according to the MD run. The deviations of the $^{h3}J_{NC'}$ values calculated from the low-resolution structure 1pga correlate strongly to the deviations of the r_{HO} distance between the low- and high-resolution structures: too small or too large r_{HO} distances in 1pga correspond to too strong or too weak predicted

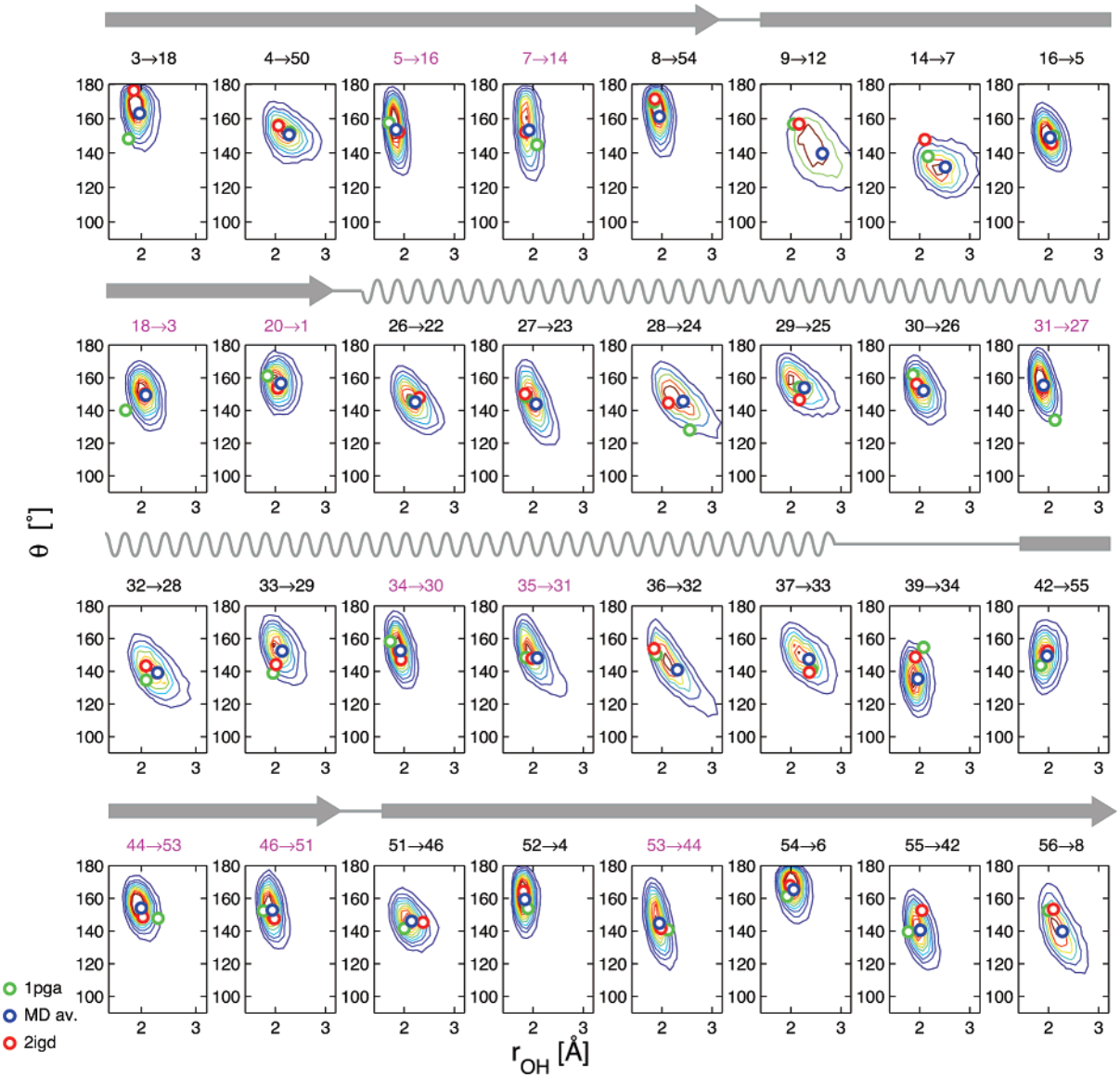

Figure 4. Histograms of H-bond geometries populated during the MD run in explicit water for protein G. Two-dimensional histograms are calculated for the populations of H-bond angles θ and H-bond distances r_{OH} in individual H-bonds. (○) θ and r_{HO} values according to the static X-ray structures 1pga (green) and 2igd (red) as well as the average over the MD run (blue). Secondary structure elements are shown at the top of the individual histograms. H-bonds highlighted in magenta have particularly strong deviations between predicted and measured $^{h3}J_{NC'}$ values for the low-resolution structure 1pga (see Figure 3).

$^{h3}J_{NC'}$ values, respectively. An analysis of the r_{HO} distances in 1pga shows that most H-bonds in the antiparallel $\beta1/\beta2$-sheet and two H-bonds at the end of the helix are too short (Y3→T18, L5→T16, T18→Y3, A20→M1, A34→F30, N35→K31), H-bond K31→E27 at the beginning of the helix is too long and twisted, and H-bonds in the antiparallel $\beta3/\beta4$-sheet are either too short (D46→T51) or too long (T44→T53, T53→T44). In all cases, the MD averaging moves the r_{HO} distances closer to the values of the 2igd structure, such that the predicted $^{h3}J_{NC'}$ coincide much better with the experimental values. Apparently, the MD averaging releases some inherent strain within the respective secondary structure elements.

Comparison of Explicit/Implicit Water. In contrast to protein G and ubiquitin, MD averaging with explicit water on the Tudor SMN domain improved the agreement between published experimental data[7] and theoretical $^{h3}J_{NC'}$ values only marginally. Thus the rmsd decreased only slightly from 0.325 Hz for the static X-ray structure (1mhn, 1.8 Å resolution) to 0.296 Hz for the MD average (Table 1). This is at variance with a reported drop from 0.35 Hz for the static structure to 0.04 Hz for the MD average using an implicit water model (generalized Born potential) and DFT-derived *J*-values.[7] It was therefore tested whether the different water models would be the source of the differing behavior. Indeed, when the generalized Born potential[9] was used as an implicit water model for the MD dynamics calculation, the rmsd decreased much further to 0.067 Hz (Table 1). No significant difference was found when the SASA (solvent-accessible surface area) model[10] was used for implicit water modeling (rmsd 0.074 Hz, Table 1). The influence of implicit water in the MD simulations was also tested for ubiquitin (Figure 5A) and protein G (Figure 5B). In both cases, the implicit water model (generalized Born) severely deteriorated the agreement to the experiment (rmsd 0.287 Hz

(9) Tsui, V.; Case, D. A. *J. Am. Chem. Soc.* **2000**, *122*, 2489−2498.
(10) Ferrara, P.; Apostolakis, J.; Caflisch, A. *Proteins: Struct., Funct., Genet.* **2002**, *46*, 24−33.

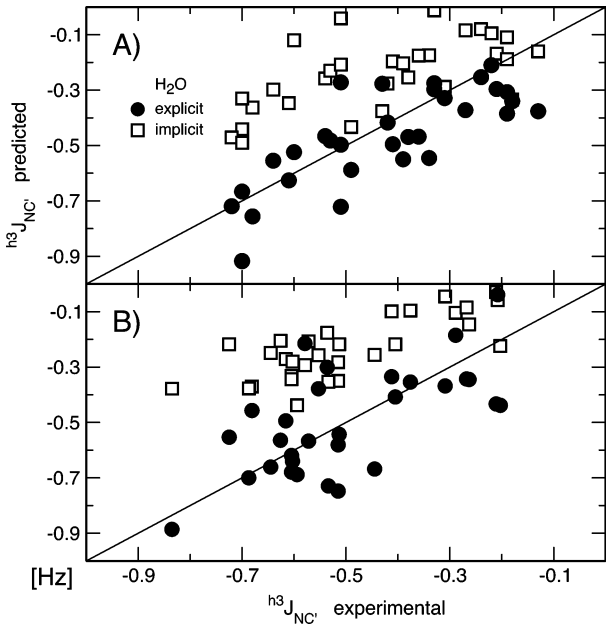

Figure 5. Comparison of the accuracy of $^{h3}J_{NC'}$ predictions derived from MD runs using either explicit or implicit water solvation. $^{h3}J_{NC'}$ values were calculated as averaged according to eq 1. (●) Explicit water solvation; (□) implicit water solvation (generalized Born model). (A) Protein G, (B) ubiquitin.

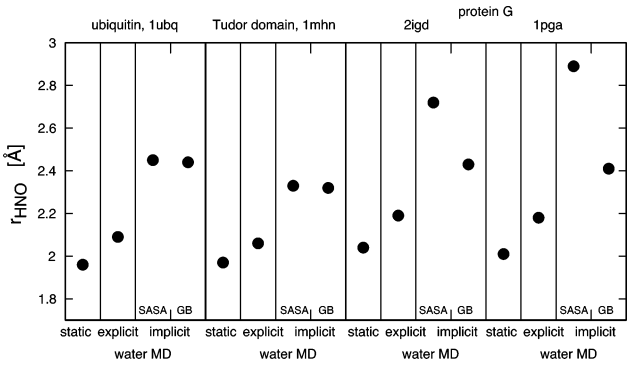

Figure 6. Average r_{HO} distances for the H-bonds in ubiquitin, protein G, and the Tudor domain. For each protein, averages are shown according to the static crystal structure, the MD trajectory with explicit water solvation, and the MD trajectory with implicit water solvation (generalized Born model and SASA model). Implicit water solvation significantly increases the r_{HO} distance in all cases.

for ubiquitin and 0.275 Hz for protein G; Table 1). Apparently, the implicit water model severely affects the average H-bond geometries.

To obtain insight into this phenomenon, the average of the H^N-O distance r_{HO} was calculated for the static structures and the dynamically averaged structures under both explicit and implicit water modeling. Figure 6 shows that the explicit water increases the average H^N-O distance by about 0.1 Å as compared to the static X-ray structures. In contrast, both implicit water models increase this distance much more, i.e. by 0.4−0.8 Å for the three different protein structures. Since the X-ray structure of the Tudor domain has standard average H-bond distances of about 2.0 Å, the likely explanation for the particular findings on the Tudor domain was an underestimation of the absolute size of the experimental $^{h3}J_{NC'}$ values. In fact, average experimental $^{h3}J_{NC'}$ values in β-sheets are -0.53 ± 0.15 Hz for ubiquitin and protein G,[3] whereas the average of the reported $^{h3}J_{NC'}$ values in the all-β-sheet Tudor domain is -0.30 ± 0.06 Hz. An increase in the H-bond lengths during the MD run will decrease the predicted $^{h3}J_{NC'}$ such that the agreement with experimental data improves.

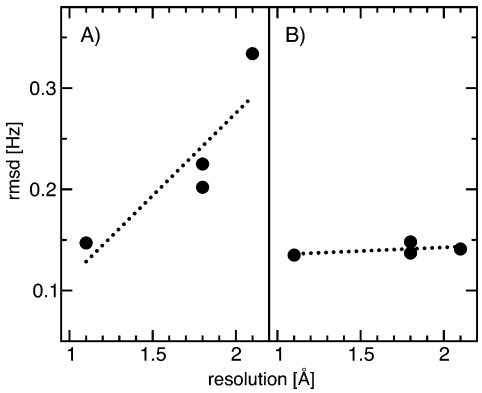

Figure 7. Root-mean-square deviations between calculated and measured $^{h3}J_{NC'}$ values in relation to the resolution of the crystal structures. (●) Data for ubiquitin (1ubq), protein G (1pga and 2igd), and the Tudor domain (1mhn, $^{h3}J_{NC'}$ rescaled); (···) linear fits to the data points. (A) $^{h3}J_{NC'}$ values were calculated from the static X-ray coordinates by eq 1. (B) $^{h3}J_{NC'}$ values were obtained by averaging over MD trajectories with explicit water solvation.

A reexamination of the original experimental data (M. Sattler, personal communication) showed that the absolute size of the $^{h3}J_{NC'}$ values had indeed been underestimated by a factor of 2. Rescaling the data (Table 1, column Tudor domain 2) gives then behavior very similar to that of the other two proteins. Thus the static structure yields an rmsd of 0.225 Hz, which drops to a value of 0.148 Hz when MD averaging with explicit water is used, but which increases to about 0.32 Hz for the MD simulations using implicit water models.

Conclusion

In summary, we could show that the accuracy of the prediction of $^{h3}J_{NC'}$ values from static structures depends monotonically on the resolution of the respective X-ray structures. Figure 7A shows this monotonic dependence. For lower resolution structures, averaging over MD trajectories with explicit solvent water significantly improves the accuracy to a value that is close to the highest resolution static X-ray structure (1.1 Å, 2igd, Figure 7B). Thus, it is not necessary to invoke dynamics to explain experimental $^{h3}J_{NC'}$ values from the present data. It may, however, be possible to improve the accuracy of the dynamical averaging further by more extended MD sampling (P. R. L. Markwick, personal communication). Yet, it remains to be explored whether even higher resolution (<1.1 Å) or better-refined static structures would not yield similar further improvements.

The improvement by MD averaging for the lower resolution structures results from a move of the average r_{HO} distances and H···O=C angles toward their respective values in the high-resolution structure. This indicates that the MD potential energy functions are highly accurate and that MD averaging with explicit water, but not with implicit water, can be used to optimize H-bond geometry. In contrast, a direct optimization against the MD potential energies did not yield improved agreement with experimental data.

In practice, the much simpler geometrical parametrization (eq 1 or 2) yields identical results to DFT calculations even for MD averaging of $^{h3}J_{NC'}$ values. The good correlation between

measured and predicted $^{h3}J_{NC'}$ values for the high-resolution structure shows that the *J*-couplings can be used as an indicator for structural quality. Vice versa, $^{h3}J_{NC'}$ couplings can be incorporated easily as restraints into structure calculations by such analytical parametrizations. In fact, $^{h3}J_{NC'}$ couplings have been used as restraints via a simple exponential distance law for the determination of the high-resolution NMR structure of ubiquitin (PDB code 1d3z),[11] and very recently by eq 1 as ensemble-averaged restraints in molecular dynamics simulations of ubiquitin and protein G.[12]

Methods

Protons were attached to the structures of the proteins ubiquitin (1ubq), protein G (1pga and 2igd), and SMN Tudor domain (1mhn) using X-PLOR[13] standard protocols. Explicit water molecular dynamics (MD) simulations were performed with NAMD 2.5[14] with the CHARMM force field at 300 K and Nosé-Hoover Langevin pressure control with periodic boundary condition. The amount of water molecules added corresponds to a hydration shell of about 8 Å thickness. The particle mesh Ewald electrostatics method was used in combination with a nonbonded interaction cutoff of 12 Å. MD production runs were carried out with time steps of 1 fs after a 2000-step energy minimization and a 50-ps equilibration. Dynamics trajectories were sampled at 0.1-ps intervals. The H-bond coordinates were extracted from these trajectories and used for the calculation of $^{h3}J_{NC'}$ values either by the geometrical formula (eq 1) or by density functional theory (DFT) (GAUSSIAN 03[15] at the UB3PW91/6-311G** level). The latter calculations were carried out on formamide dimers oriented according to the H-bond geometry of the corresponding amino acid pairs.

MD simulations with implicit water were carried out by use of the generalized Born (GB) solvation model[9] implemented in AMBER[16] or the solvent-accessible surface area (SASA) model[10] implemented in CHARMM.[17] The MD trajectories were sampled at 0.1-ps intervals after energy minimization, heating, and equilibration periods of 50 ps each, as described previously.[7]

Acknowledgment. We thank Professor M. Meuwly for very valuable discussions and help with setting up the CHARMM calculations. We also thank Professor M. Sattler, Dr. P. R. L. Markwick, and Dr. R. Sprangers for very collegial and stimulating discussions and for making information on the improved Tudor domain data available to us. This work was supported by SNF Grant 31-109712 (S.G.).

Supporting Information Available: Complete refs 15 and 16. This material is available free of charge via the Internet at http://pubs.acs.org.

JA068336H

(11) Cornilescu, G.; Marquardt, J. L.; Ottiger, M.; Bax, A. *J. Am. Chem. Soc.* **1998**, *120*, 6836−6837.
(12) Gsponer, J.; Hopearuoho, H.; Cavalli, A.; Dobson, C. M.; Vendruscolo, M. *J. Am. Chem. Soc.* **2006**, *128*, 15127−15135.
(13) Brünger, A. X-PLOR Version 3.1: A system for Crystallography and NMR; Yale University: New Haven, CT, 1992.
(14) Phillips, J. C.; Braun, R.; Wang, W.; Gumbart, J.; Tajkhorshid, E.; Villa, E.; Chipot, C.; Skeel, R. D.; Kale, L.; Schulten, K. *J. Comput. Chem.* **2005**, *26*, 1781−1802.
(15) Frisch, M. J.; et al. Gaussian 03, Revision B.03; Gaussian Inc: Pittsburgh PA, 2003.
(16) Case, D. A.; et al. AMBER 7; University of California: San Francisco, 2002.
(17) Brooks, B. R.; Bruccoleri, R. E.; Olafson, B. D.; States, D. J.; Swaminathan, S.; Karplus, M. *J. Comput. Chem.* **1983**, *4*, 187−217.